UC Berkeley
UC Berkeley Previously Published Works

Title
Co-occurrence of Photochemical and Microbiological Transformation Processes in Open-Water Unit Process Wetlands

Permalink
https://escholarship.org/uc/item/02w980xj

Journal
Environmental Science and Technology, 49(24)

ISSN
0013-936X

Authors
Prasse, Carsten
Wenk, Jannis
Jasper, Justin T
et al.

Publication Date
2015-12-15

DOI
10.1021/acs.est.5b03783

Peer reviewed

Co-occurrence of Photochemical and Microbiological Transformation Processes in Open-Water Unit Process Wetlands

Carsten Prasse[1,2], Jannis Wenk[1,3,#], Justin T. Jasper[1],
Thomas A. Ternes[2], David L. Sedlak[1,*]

[1] ReNUWIt Engineering Research Center and Department of Civil & Environmental Engineering, University of California at Berkeley, Berkeley, California 94720, United States
[2] Department of Aquatic Chemistry, Federal Institute of Hydrology (BfG), Koblenz, Germany
[3] Department of Chemical Engineering and Water Innovation & Research Centre (WIRC), University of Bath, Claverton Down, Bath BA2 7AY, United Kingdom

* Corresponding author: sedlak@berkeley.edu

Co-occurrence of Photochemical and Microbiological Transformation Processes in Open-Water Unit Process Wetlands
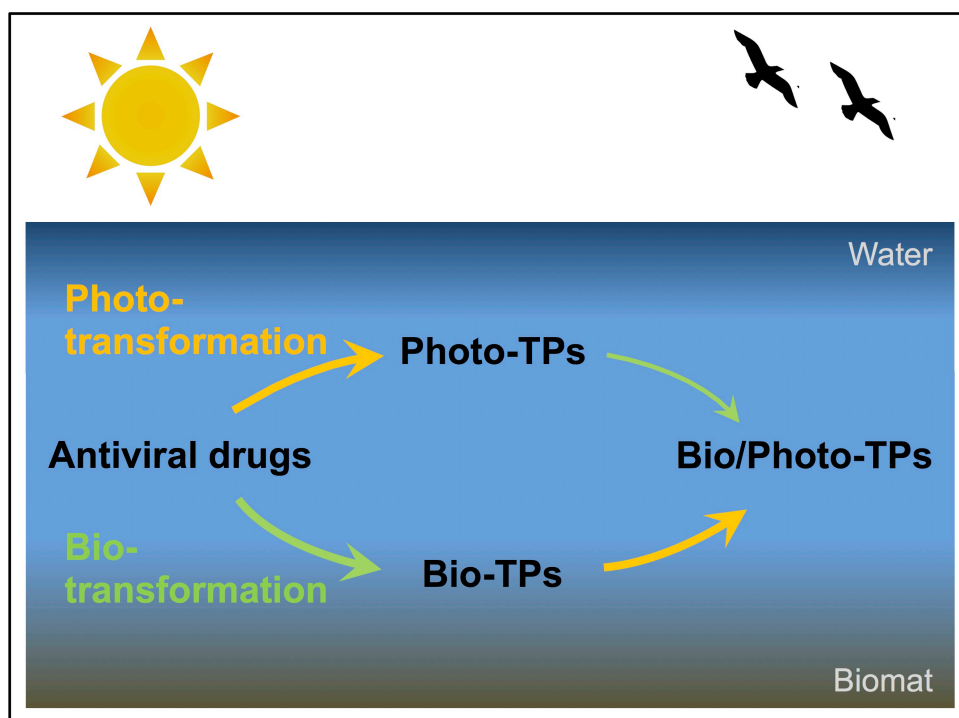
Carsten Prasse[1,2], Jannis Wenk[1,3], Justin T. Jasper[1], Thomas A. Ternes[2], David L. Sedlak[1*]

[1] ReNUWIt Engineering Research Center and Department of Civil & Environmental Engineering, University of California at Berkeley, Berkeley, California 94720, United States

[2] Department of Aquatic Chemistry, Federal Institute of Hydrology (BfG), Koblenz, Germany

[3] Department of Chemical Engineering and Water Innovation & Research Centre (WIRC), University of Bath, Claverton Down, Bath BA2 7AY, United Kingdom

*Corresponding author: sedlak@berkeley.edu

Abstract

The fate of anthropogenic trace organic contaminants in surface waters can be complex due to the occurrence of multiple parallel and consecutive transformation processes. In this study, the removal of five antiviral drugs (i.e., abacavir, acyclovir, emtricitabine, lamivudine and zidovudine) via both bio- and photo-transformation processes was investigated in laboratory microcosm experiments simulating an open-water unit process wetland receiving municipal wastewater effluent. Phototransformation was the main removal mechanism for abacavir, zidovudine and emtricitabine, with half-lives ($t_{1/2,photo}$) in wetland water of 1.6 h, 7.6 h and 25 h, respectively. In contrast, removal of acyclovir and lamivudine was mainly attributable to slower microbial processes ($t_{1/2,bio}$ = 74 h and 120 h, respectively). Identification of transformation products revealed that bio- and photo-transformation reactions took place at different moieties. For abacavir and zidovudine, rapid transformation was attributable to the high reactivity of the cyclopropylamine and azido moiety, respectively. Despite substantial differences in kinetics of different antiviral drugs, biotransformation reactions mainly involved oxidation of hydroxyl groups to the corresponding carboxylic acids. Phototransformation rates of parent antiviral drugs and their biotransformation products were similar, indicating that prior exposure to microorganisms (e.g., in a wastewater treatment plant or a vegetated wetland) would not affect the rate of transformation of the part of the molecule that was susceptible to phototransformation. However, phototransformation strongly affected the rates of biotransformation of the hydroxyl groups, which, in some cases, resulted in greater persistence of phototransformation products.

3

Introduction

The discharge of municipal wastewater effluents into surface waters can result in the presence of trace organic contaminants at concentrations that pose potential risks to aquatic ecosystems and drinking water resources. After their release, many trace organic contaminants are attenuated by biological and photochemical processes. Although these processes often occur simultaneously or sequentially in the environment, most studies have considered the occurrence of only one transformation process at a time.[1-4] Thus, it is difficult to predict which transformation products will be formed and whether or not transformation reactions occurring at one moiety alter the kinetics of subsequent transformation reactions. Furthermore, if partial transformation of a compound enhances the reactivity of other moieties, interaction of transformation processes could result in changes in the distribution of transformation products as well as their rates of removal. For example, carbamazepine, a compound that is particularly resistant to biotransformation is slowly transformed upon exposure to sunlight via direct photolysis and reaction with $^\bullet$OH.[5,6] This leads to the formation hydroxylated derivatives,[7] which are more easily biodegraded than the parent compound.[8]

Open water unit process wetlands have been developed as a polishing treatment step for municipal wastewater effluents.[9] These managed natural systems utilize sunlight to remove trace organic compounds and inactivate pathogens.[10-12] In addition, microorganisms in the biomat formed at the bottom of these treatment basins reduce nitrate and contribute to aerobic biodegradation of trace organic contaminants.[13,14] To assess the importance of the co-occurrence of biological and photochemical transformation reactions to reaction kinetics and product distribution, the fate of five antiviral drugs (i.e., abacavir, emtricitabine, lamivudine, zidovudine and acyclovir, see Figure 1) was studied under conditions comparable to those encountered in open-water unit process wetlands.

Antiviral drugs were chosen because they are widely used for the treatment of diseases such as herpes, hepatitis and HIV, and have been detected at concentrations above 1 µg L^{-1} in municipal wastewater effluents.[15-18] No information about potential environmental effects resulting from the release of these compound into the aquatic environment is available so far. Furthermore, little is known about the effects of these compounds on

82 environmental viruses, a group of microorganisms that play a very important role in

83 aquatic ecosystems.[19]

84 By investigating transformation kinetics and transformation mechanisms under conditions

85 comparable to those encountered in open-water unit process wetlands it is possible to gain

86 insight into how simultaneously occurring bio- and photo-transformation reactions affect

87 the overall fate of antiviral drugs in sunlit surface waters. These compounds also serve as

88 models for other families of compounds that contain moieties that are susceptible to bio-
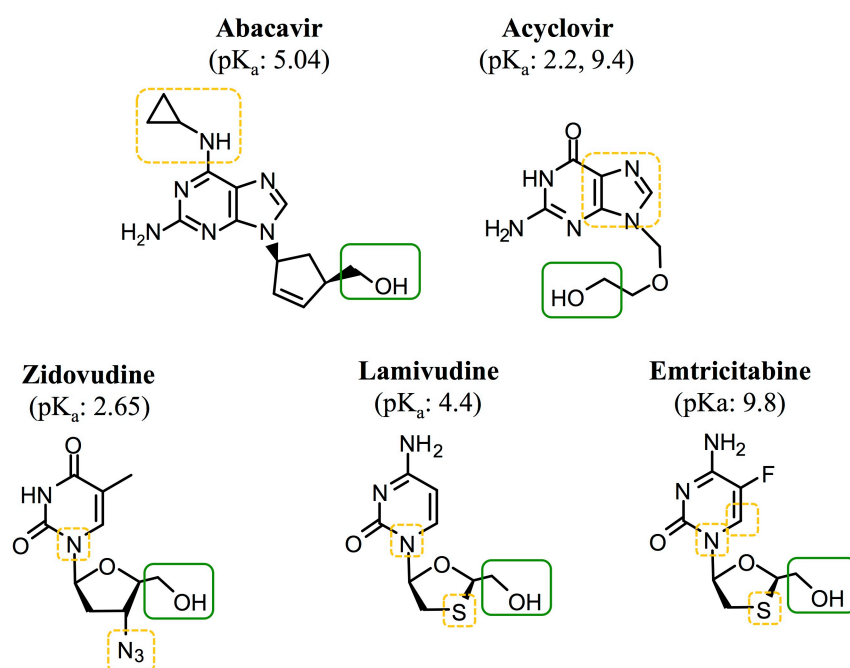
89 and phototransformation.

90

Figure 1. *Antiviral drugs and their most likely sites of proposed photo- (▢) and biotransformation (▢) reactions.*

91

Materials and Methods

Chemicals

Analytical reference standards of antiviral drugs and stable isotope-labeled analogues used as internal standards (purity > 99%) were purchased from Toronto Research Chemicals (Ontario, Canada). All other chemicals and solvents were obtained from Fisher Scientific (Fairlawn, NJ).

5

98

Wetland water sampling conditions

Phototransformation experiments were conducted in water collected from a pilot-scale open-water unit process wetland located in Discovery Bay, CA. The facility treats about 10,000 gallons per day (4.4×10^{-4} m^3 s^{-1}) of nitrified wastewater effluent from an adjacent municipal wastewater treatment plant. Details about the open-water unit process wetland were described previously.[10,13] Water collected from the open-water wetland typically contained 10 - 20 mg L^{-1} -N NO$_3^-$, 5 - 10 mg L^{-1}-C DOC, and 60 - 80 mg L^{-1}-C dissolved inorganic carbon (HCO$_3^-$ and CO$_3^{2-}$). Samples for laboratory irradiation experiments were collected from the mid-point of the wetland. All samples were filtered through pre-rinsed 1μm (nominal pore size) glass fiber filters (Whatman) and were stored in the dark at 4°C until analysis, which occurred within 5 days.

Laboratory photo- and biotransformation experiments

Irradiation experiments were performed using a collimated beam Oriel Solar Simulator (Spectra Physics, serial no. 91194) equipped with a 1000 W Xe lamp and either two successive atmospheric attenuation filters (Spectra Physics, serial no. 81088 & 81017) or one atmospheric and one UVB-filter (Spectra Physics, serial no. 81088 & 81050). Spectral irradiance was routinely measured with a spectroradiometer (RPS 380, International light) at different locations of the irradiated area to assess variability, which was always < 5%. Details on lamp irradiance energies and the spectra of different configurations are given in section 1.1 of the Supporting Information (SI). Irradiation experiments were carried out in 100 mL black-painted glass beakers that were placed in a water bath at constant temperature (18 ± 2°C). Initial concentrations of antivirals of approximately 0.5 μM were used for all kinetics experiments. Pseudo-first order phototransformation rate constants of antivirals and photochemical probe compounds used for the quantification of concentrations of reactive intermediates were calculated from the slopes of linear regression of the natural log of concentration versus time. No degradation of antiviral drugs was observed in control experiments in the dark indicating that their transformation in filtered wetland water was only attributable to photochemical processes.

6

128 For the elucidation of biotransformation kinetics, beakers were additionally supplemented

129 with 10 mL of the biomat taken from the bottom of a pilot-scale open-water wetland and

130 kept in the dark (see Jasper et al.[13] for further details). Biodegradation of compounds

131 followed pseudo-first order degradation kinetics, indicating stable conditions throughout

132 the experiments. In addition, observed transformation rates in good agreement with

133 results from a preliminary study used to design the more detailed experiments.

134

135 *Direct and indirect phototransformation.* Experiments to assess direct phototransformation

136 of antiviral drugs were conducted in buffered ultrapure water at pH-values ranging from 6

137 to 10 (pH 6 - 8: 5 mM phosphate buffer; pH 9 - 10: 5 mM borate buffer). Samples (1 mL)

138 were collected at regular time intervals and stored at 4°C in the dark until analysis.

139 Electronic absorption spectra of antiviral drugs at different pH values (see Fig. S2) were

140 recorded with a UV-2600 UV-Vis Spectrophotometer (Shimadzu) using quartz-glass

141 cuvettes (Hellma, Germany). Further details on determination of quantum yields using the

142 *p*-nitroanisole (PNA)/pyridine(PYR) method[20] and related calculations are provided in

143 section 1.6 of the SI.

144 Indirect phototransformation of antiviral drugs was investigated by the addition of specific

145 quenchers to wetland water: *N,N*-dimethylaniline (DMA; 10 μM) was used to scavenge CO_3-

146 radicals[10], sorbic acid (2.5 mM) was used to scavenge excited triplet states of the dissolved

147 organic matter ($^3DOM^*$)[21], histidine (20 mM) was used to scavenge singlet oxygen ($^1O_2$)[22]

148 and isopropyl alcohol (IPA; 26 mM) was used to scavenge $^\bullet OH$-radicals.[23] In addition,

149 experiments with specific photosensitizers were conducted in ultrapure buffered water to

150 determine reaction rate constants of antiviral drugs with individual reactive intermediates:

151 For $CO_3^{-\bullet}$, either $NaNO_3/NaHCO_3$ or duroquinone/$NaHCO_3$ photosensitizer methods were

152 used.[24,25] The excited triplet state photosensitizers 3-methoxyacetophenone (3MAP) and

153 anthraquinone-2-sulfonate (AQ2S) served as proxies for $^3DOM^*$.[26] Hydroxyl-radicals were

154 generated by the irradiation of $NaNO_3$ solutions.[27] For $^1O_2$ production, Rose Bengal was

155 used as a photosensitizer.[28] To further verify the role of $^1O_2$, some experiments were

156 performed in D_2O. Reaction rate constants were either determined by competition kinetics

157 or by comparing reaction rates of antiviral drugs with those of established photochemical

158 probe compounds (experimental details and calculations are provided in section 1.5 and

7

159 1.7). For all indirect phototransformation experiments, the concentration changes of
160 photochemical probe compounds and antiviral drugs during irradiations were determined
161 by HPLC-UV. Experimental and analytical details, including comprehensive results are
162 provided in the SI section 1.2.

163 Given the structural similarities of antivirals with DNA bases, additional irradiation
164 experiments were performed with adenine, 2-amino adenosine, cytosine, cytidine, guanine,
165 thymidine and thymine (SI section 2.1.1) to obtain further information about the
166 photoreactive moieties in the molecules to aid the identification of transformation
167 products.

168

169 *Identification of photo- and biotransformation products.* High resolution mass spectrometry
170 (HR-MS; LTQ Orbitrap Velos, Thermo Scientific, Bremen, Germany) was used to conduct
171 accurate MS and MS/MS analysis of transformation products of antiviral drugs. To this end,
172 experiments at elevated concentrations (40 µM) were used. The LTQ Orbitrap Velos was
173 coupled to a Thermo Scientific Accela liquid chromatography system (Accela pump and
174 autosampler). HR-MS was conducted in the positive electrospray ionization (ESI) mode. To
175 obtain information on the chemical structure of the TPs, MS^n fragmentation experiments
176 were conducted using data-dependent acquisition. Further information on the applied
177 setup and data dependent acquisition parameters can be found in the SI (section 1.3).
178 Product formation of antiviral drugs in laboratory experiments was determined by liquid
179 chromatography tandem mass spectrometry (LC/MS/MS). Details are provided in the SI
180 (section 1.4).

181

182 *Combined bio- and photodegradation experiments.* The fate of antiviral drugs in the
183 presence of sunlight and microorganisms was investigated over a 72 h period in the
184 laboratory. Black-painted glass beakers (250mL) were filled with 180 mL of wetland water
185 and 20 mL of freshly collected biomat material from the bottom of the Discovery Bay open-
186 water unit process wetland. The experimental setup was the same as described above for
187 photochemical experiments, but with three day/night cycles to simulate field conditions (8
188 h of daily irradiation followed by 16 h in the darkness; 72 h total). Antiviral drugs were
189 added individually at concentrations of 0.5 µM to ensure detection of both parent antiviral

190 compounds and their transformation products. Samples were collected at regular time

191 intervals and stored at 4°C in the dark prior to LC/MS/MS analysis, which occurred within

192 24 h. Further details about the analytical method can be found in the SI.

193

194 **Results and Discussion**

195 *Phototransformation in wetland water*

196 Phototransformation of the five investigated antiviral drugs in wetland water followed

197 first-order kinetics ($r^2 \geq 0.98$; Figure S4-S8). In native wetland water (pH 8.9), the fastest

198 phototransformation was observed for abacavir ($k_{obs} = 0.52 \pm 0.06$ h^{-1}), zidovudine ($k_{obs} =$

199 0.09 ± 0.002 h^{-1}) and emtricitabine ($k_{obs} = 0.03 \pm 0.002$ h^{-1}) whereas the transformation of

200 acyclovir and lamivudine were significantly slower ($k_{obs} = 0.012 \pm 0.001$ h^{-1} and $0.011 \pm$

201 0.001 h^{-1}, respectively) (Figure 2). No degradation of antiviral drugs in wetland water

202 occurred in the dark indicating that their removal was solely attributable to photochemical

203 processes. Photosynthetic activity leads to significant diurnal fluctuations of pH in open-

204 surface wetlands.[10] Therefore, phototransformation kinetics of antiviral drugs in wetland

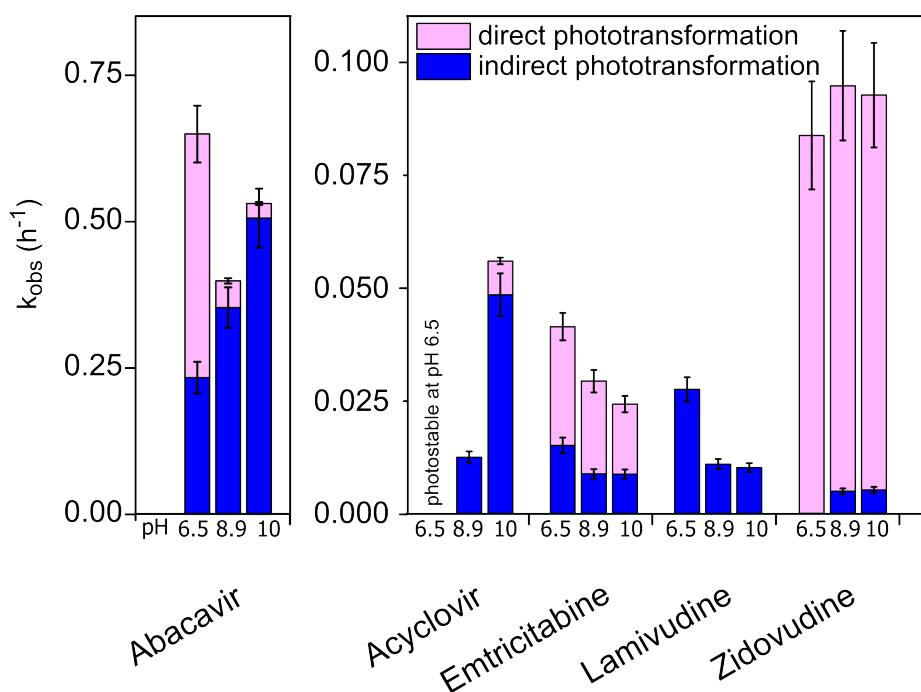205 water were also determined at pH 6.5 and pH 10 (Figure 2).

206

Figure 2. Phototransformation kinetics of antiviral drugs in experiments with

9

207

208   Phototransformation of abacavir in wetland water increased when the pH value was

209   adjusted to 6.5 or 10. This can be attributed to a higher contribution of direct photolysis

210   due to higher quantum yields at lower pH values (i.e., Φ_{app} is 4.2 to 11.4 times higher

211   between pH 6 – 8, compared to pH 9 and 10, SI Table S5) and faster indirect photolysis at

212   higher pH values. Comparison of transformation kinetics with results obtained in ultrapure

213   water revealed the dominance of indirect photodegradation processes at pH 8.9 and 10,

214   whereas direct photolysis was more important at pH 6.5. The addition of sorbic acid and

215   histidine significantly reduced phototransformation rates of abacavir in wetland water

216   (Fig. S4). Although interpretation of results from experiments with scavengers requires

217   caution,[29] these results suggest the involvement of $^3DOM^*$ and $^1O_2$ in the photochemical fate

218   of this compound. This was also supported by experiments with specific singlet oxygen and

219   excited triplet state sensitizers (see below). Negligible removal of the structural analogues

220   adenine and 2-amino-adenosine further indicated that the photolability of abacavir can be

221   attributed to the cyclopropyl-moiety (see SI section 2.1.1).

222   Rates of phototransformation of zidovudine were not affected by changes in pH.

223   Comparison with reaction rates in both ultrapure water and wetland water in the presence

224   of scavengers revealed the dominance of direct photolysis (Fig. S5). Similar to abacavir,

225   comparison with the depletion of structural analogues thymine and thymidine indicated

226   that the azide moiety was responsible for the observed photoreactivity of zidovudine as

227   both analogues showed no removal when exposed to light (see SI section 2.1.1).

228   Phototransformation rates of acyclovir in wetland water increased with increasing pH.

229   Comparison with results from ultrapure water revealed that removal at pH 8.9 was solely

230   due to indirect photolysis, whereas at pH 10 direct photolysis was also important.

231   Significantly reduced rates of acyclovir phototransformation in the presence of histidine

232   and sorbic acid indicated the importance of $^1O_2$ and $^3DOM^*$ to indirect photolysis (Fig. S6).

233   In contrast to abacavir and zidovudine, phototransformation kinetics were similar to those

234   observed for the structural analogue guanine (SI Fig. S15). Thus, phototransformation of
235   acyclovir can be attributed primarily to the guanine moiety.

236   For lamivudine and emtricitabine, phototransformation kinetics in wetland water
237   decreased with increasing pH. No removal of lamivudine was observed in ultrapure water
238   indicating that its removal was entirely attributable to indirect photolysis. Higher
239   phototransformation rates of emtricitabine relative to lamivudine further indicated the
240   strong influence of the fluorine atom for emtricitabine's photolability. The presence of the
241   fluorine substituent led to greater light absorption at 300-320 nm (SI Fig. S2). Even though
242   the absorption spectrum of emtricitabine did not change with pH, the quantum yield
243   steadily decreased with increasing pH (Table S5). Phototransformation of lamivudine in
244   wetland water was fully inhibited by sorbic acid, histidine and IPA but was unaltered in the
245   presence of DMA (Fig. S7). This indicates the importance of $^3DOM^*$, $^1O_2$ and OH-radicals for
246   its indirect phototransformation. For emtricitabine, phototransformation rates in wetland
247   water were only affected by IPA and sorbic acid (Fig. S8), suggesting that reactions with $^1O_2$
248   are less important for this compound. The high photostability of its associated DNA base
249   cytosine and nucleotide cytidine revealed the importance of structural modifications (thiol
250   group (both compounds) and fluorine (emtricitabine) to the observed photodegradation.

251

252   Additional experiments with individual reactive species revealed second-order reaction
253   rates with $^\bullet OH$ at or above (abacavir, zidovudine) diffusion controlled rates ranging from
254    $5 \cdot 10^9$ to $1.1 \cdot 10^{11}$ $M^{-1}s^{-1}$ (Table 1). Antiviral compounds were reactive with $CO_3^{\bullet-}$, at rates
255   between $1.2 \cdot 10^6$ and $1.2 \cdot 10^9$ $M^{-1}s^{-1}$, while only abacavir ($1.2 \cdot 10^9$ $M^{-1}s^{-1}$) and acyclovir
256   ($1.2 \cdot 10^7$ $M^{-1}s^{-1}$) reacted with $^1O_2$. With the exception of abacavir, no depletion of antiviral
257   compounds was observed in the presence of the model triplet photosensitizer 3MAP.
258   However depletion of all compounds was observed in the presence of AQ2S at rates similar
259   to or higher than the reference probe compound TMP, indicating selective reactivity with
260   excited triplet states. Comparison of measured and predicted rate constant for antivirals
261   under wetland conditions (obtained by multiplication of steady-state concentrations of
262   reactive species measured in wetland water with measured second-order reaction rate
263   constants of antivirals with $^1O_2$, $^\bullet OH$ and $^\bullet CO_3^-$) were in good agreement, indicating
264   reasonable results.

Table 1. Quantum yields (pH 9) and apparent second-order reaction rate constants of indirect phototransformation of antiviral drugs via reaction with $^1O_2$, $^\bullet OH$, $^\bullet CO_3^-$ and excited triplet states (given relative to the degradation of the $^3Sens^*$ probe compound TMP). Quantum yields of antiviral drugs at pH 6-8 and pH 10 can be found in SI Table S5.

	[M Es^{-1}]	[M^{-1} s^{-1}]				[-]	
	$\Phi_{app(300-400nm)}$ (pH 9)	$^1O_2$	$^\bullet OH$	$^\bullet CO_3^-$ (NO$_3^-$ + HCO$_3^-$/CO$_3^{2-}$)	$^\bullet CO_3^-$ (DQ)	$^3SENS^*$ (AQ2S)	$^3SENS^*$ (MAP)
Abacavir	0.014 (±0.003)	1.2 x 10^9 (± 18%)	1.1 x 10^{11} (± 3%)	1.2 x 10^9 (± 4%)	-[a]	4.88	13.5
Zidovudine	0.45 (±0.15)	n.d.	1.3 x 10^{10} (± 2%)	2.4 x 10^6 (± 5%)	1.3 x 10^6 (± 4%)	0.62	n.d.
Acyclovir	0.01 (±0.005)	1.2 x 10^7 (± 25%)	5.0 x 10^9 (± 2%)	1.2 x 10^8 (± 2%)	6.3 x 10^7 (± 4%)	0.08	n.d.
Emtricitabine	0.016 (±0.005)	n.d.	9.3 x 10^9 (± 2%)	3.0 x 10^6 (± 4%)	4.3 x 10^6 (± 12%)	2.03	n.d.
Lamivudine	n.d.	n.d.	9.2 x 10^9 (± 1%)	1.2 x 10^6 (± 3%)	1.7 x 10^6 (± 3%)	1.86	n.d.

268   n.d.: not detected above level of uncertainty; [a] not applicable due to reaction of abacavir with DQ in the dark

269

Comparison of photo- vs biotransformation rates

Dark experiments conducted with wetland water in the presence of biomat material indicated that biotransformation rates varied considerably among antiviral drugs. Biotransformation half-life times ($t_{1/2,bio}$) ranged from 74 h for acyclovir to 500 h (21 d) for emtricitabine (Fig. 3; Fig. S13). Under typical wetland treatment conditions (i.e., hydraulic retention times of 2-3 days), significant biological attenuation of acyclovir and abacavir is expected whereas removal of the other antiviral drugs via microbial processes is unlikely to be important. Comparison of transformation rates of antiviral drugs in the dark to those observed in irradiated wetland water indicated that phototransformation processes were dominant for abacavir, zidovudine and emtricitabine, while for acyclovir and lamivudine biotransformation was similar or more important than photolysis during typical summertime conditions (Fig. 3).
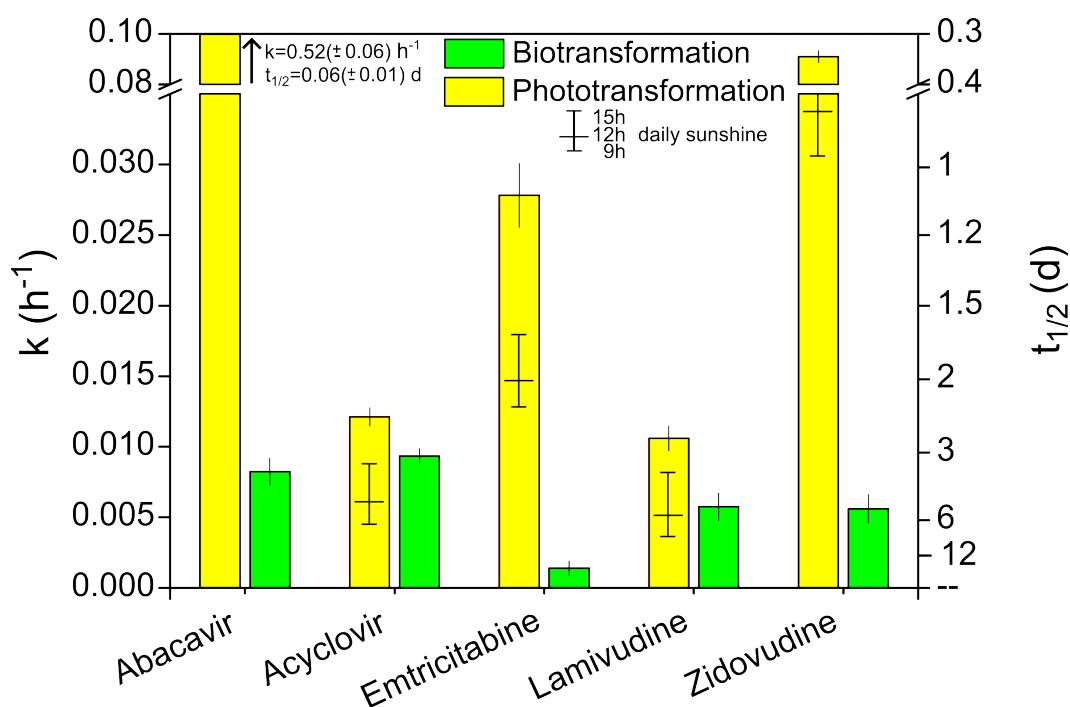
282

Figure 3. Photo- and biotransformation rate constants k (h^{-1}) and associated half-life time $t_{1/2}$ (d) of antiviral drugs in laboratory experiments. Small bars within phototransformation columns indicate half-life times based on daily sunshine hours (9-15 hours). For the determination of biodegradation half-life times, experiments were conducted in the presence of the biomat in the dark. Error bars represent 95% confidence intervals obtained from linear regressions.

283

Transformation of abacavir

284

HRMS analysis indicated that four primary transformation products (TP318, TP288, TP284 and TP246) were formed during photolysis of abacavir in wetland water (SI section 2.2; Table S7). In agreement with results obtained for the structural analogues 2-amino-adenosine and adenine, fragmentation patterns of TP318, TP288 and TP246 revealed that the cyclopropylamine moiety was the main site of reaction, leaving the 2-amino-adenine (fragments: m/z 151.073, 134.046 and 109.051) and the 2-cyclopenten-1-methanyl moieties (fragments: m/z 95.353 and 79.054) unaltered.

Exact mass calculations of TP318 showed addition of two oxygen atoms to the cyclopropyl moiety (Δm +31.9898 Da). Results from MS^2 experiments were consistent with the scission of the cyclopropyl ring and the presence of a terminal hydroxyl group, as indicated by the cleavage of H_2O and CH_2O.

For TP288, MS data suggested modification of the cyclopropyl moiety via loss of one carbon atom and the addition of one oxygen atom, leading to the formation of an acetamide,

13

298   whereas TP246 was formed via cleavage of the cyclopropyl ring. The chemical structure of

299   TP246 was confirmed by comparison with a commercially available reference standard.

300   The exact mass and fragmentation pattern of TP284 was consistent with loss of two

301   protons from either the cyclopropylamine or the 2-amino-adenosine moiety (fragments

302   m/z 149.069 and 189.088 instead of m/z 151.073 and 191.104 compared to abacavir and

303   the other TPs). Considering the high photolability of the cyclopropyl moiety, these

304   structural changes were most likely due to the formation of a cyclopropylimine.

305   To assess the relative importance of direct and different indirect photolysis processes for

306   formation of the observed abacavir transformation products, their formation was

307   investigated in buffered water (direct photolysis only), wetland water (direct and indirect

308   photolysis), and wetland water in the presence of different reactive intermediate

309   scavengers. The results revealed that both direct and indirect photolysis of abacavir

310   produced the same suite of TPs at similar relative concentrations, despite the fact that the

311   disappearance of the parent compound was significantly accelerated in the presence of

312   DOM and individual reactive intermediates (Fig. S17 & S18). Similar results have been

313   reported for irgarol, an algaecide that is structurally similar to abacavir, suggesting that the

314   cyclopropylamine moiety is the main site of reaction under all conditions.[30]

315   Photodegradation experiments in buffered ultrapure water with different optical filters

316   indicated that wavelengths below 320 nm preferentially led to cleavage of the cyclopropyl

317   moiety (TP246), whereas wavelengths above 320 nm (UV-A & visible light) led to scission

318   of the cyclopropyl ring followed by partial oxidation (TP318) (Fig. S19).

319   These findings suggest that phototransformation of abacavir is initiated by a one-electron

320   oxidation of the cyclopropylamine moiety, leading to the formation of a

321   cyclopropylaminium radical cation,[31,32] followed by subsequent reactions resulting in the

322   formation of various products. Interestingly, this phenomenon has also been utilized for

323   the investigation of electron-hopping in DNA by modifying guanine and adenine with

324   cyclopropyl moieties.[33,34] Due to the instability of the initially formed closed ring radical

325   cation, the modification results in rapid cyclopropyl ring-opening as well as 1,2-hydrogen

326   migration, leading to the formation of an ionized allylamine.[31,35] Scission of the ring is

327   followed either by a complete cleavage of the cyclopropyl moiety (TP246) or reaction of the

328   ring opened radical cation with H_2O/O_2.[33,35] In the latter case, electron release from the

14

329 carbon centered radical followed by hydrolysis leads to the formation of a 3-
330 hydroxypropanaminium cation[36] and subsequent addition of water results in the formation
331 of the 3-hydroxypropanamide (TP318). In our system, TP288 is formed by photolytic
332 cleavage of the hydroxymethyl group which leads to the formation of the acetamide
333 product.[36,37] TP284 was most likely formed via H-atom abstraction, resulting in the
334 formation of a neutral cyclopropyl radical followed by an electron transfer reaction and/or
335 hydrolysis and elimination of water even though this reaction has only been shown to be
336 catalyzed by enzymes so far.[38,39]

337

338 Experiments with biomat material in the dark to determine the relative importance of
339 biotransformation reactions indicated that microbial transformation of abacavir mainly
340 occurred via oxidation of the primary alcohol group of the 2-cyclopenten-1-
341 hydroxymethanyl side chain to produce the corresponding carboxylic acid (abacavir
342 carboxylate, Fig. S13). This was consistent with previous experiments conducted with
343 mixed liquor suspended solids from an activated sludge treatment plant.[40]

344

345 When abacavir was exposed simultaneously to light and microorganisms (Fig. 4), a rapid
346 loss of the compound was observed during the first 8-hour light period (i.e., the initial
347 concentration decreased by approximately 90 %). For the next 16 hours (i.e., the dark
348 period) abacavir removal was significantly slower. When the light was turned back on,
349 nearly all remaining abacavir disappeared. As expected, the light-induced transformation of
350 abacavir gave rise to the four photo-TPs described above (middle panel of Fig. 4). The
351 concentrations of these photo-TPs decreased by approximately 25% over the next 2.5 days,
352 indicating that further transformation took place, either via photolytic or microbial
353 processes.
354 Additional biodegradation experiments with the four photo-TPs of abacavir revealed that
355 biotransformation occurs at the same moiety as observed for the parent compound, leading
356 to the corresponding carboxylates (TP246 carboxylate, TP284 carboxylate, TP288
357 carboxylate and TP318 carboxylate; Fig. S20). Exact mass data and fragmentation patterns
358 of bio-photo TPs determined by HRMS analysis are included in section 2.2 of the SI.
359 Consequently, the observed decrease in concentration of photo-TPs shown in the middle

360 panel of Fig. 4 was mainly attributable to biotransformation, leading to a steady formation

361 of carboxylate photo-TPs (bottom panel of Fig. 4). Faster transformation rates of abacavir

362 photo-TPs observed during irradiation periods may have been attributable to enhanced

363 biotransformation due to elevated oxygen concentrations or elevated pH values that

364 occurred when photosynthetic microbes in the biomat were active. Differences in

365 biotransformation rates of TP246, TP284, TP288 and TP318, compared to abacavir (Fig.

366 S14), indicate that alteration of chemical structure influences biotransformation kinetics,

367 e.g. by affecting enzyme binding affinities or steric properties. Light-exposure of abacavir

368 carboxylate formed in the dark led to its phototransformation, ultimately yielding the same

369 photo-TPs as abacavir (bottom panel of Fig. 4). Considering that abacavir is already

370 transformed extensively to abacavir carboxylate in activated sludge treatment,[40] a rapid

371 elimination of both compounds can be expected in open-water unit process wetlands. In

372 contrast to biotransformation reactions, similar phototransformation kinetics were

373 observed for abacavir and abacavir carboxylate (Fig. S12). TP246 carboxylate was

374 identified as the main product that accumulates over time because it is not susceptible to
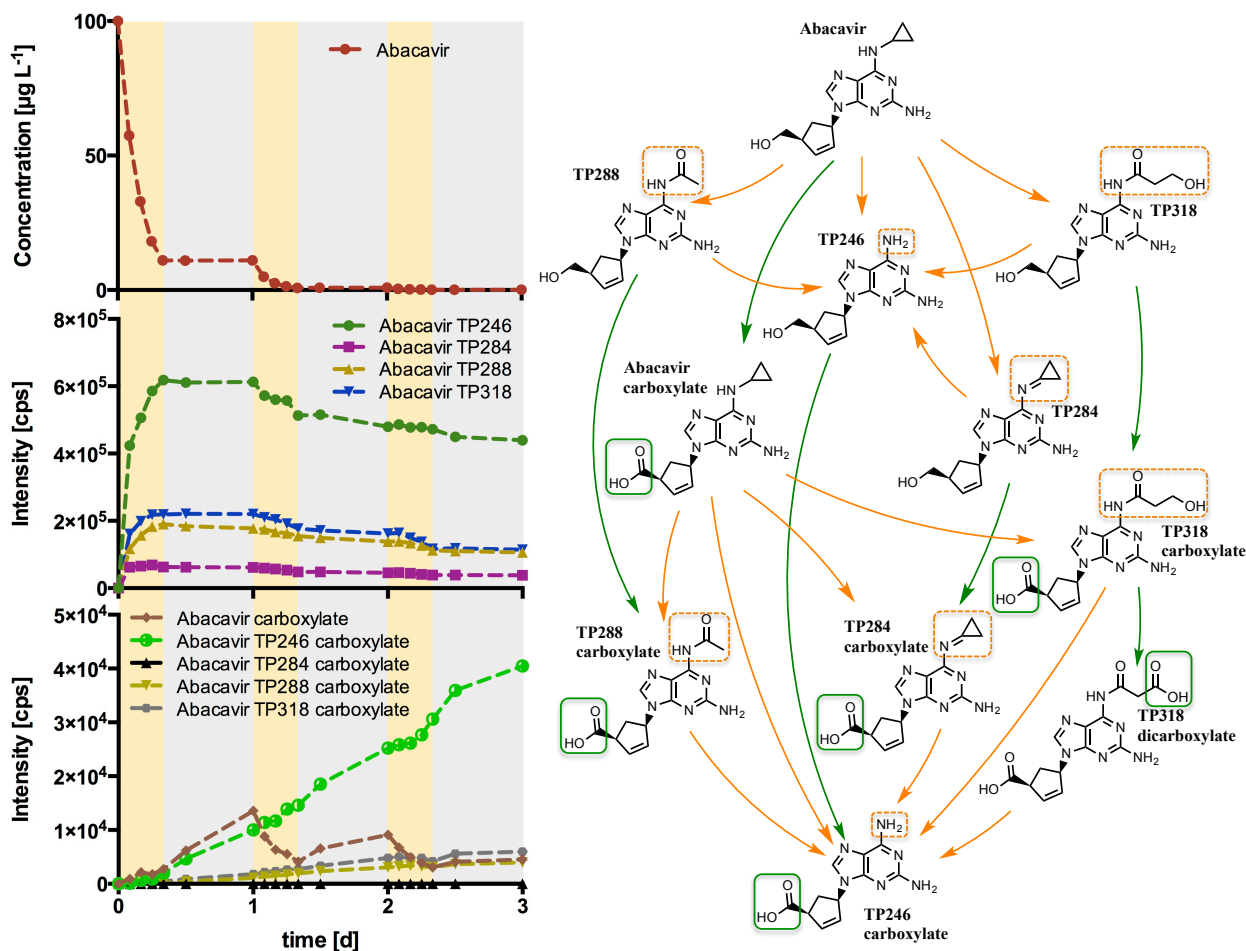
375 further reactions.

Figure 4. Transformation of abacavir (left, top) and resulting formation of photo-TPs (left, middle) and bio- / bio-photo-TPs (left, bottom)) as well as proposed transformation pathway (right) in combined in 3 day experiments in the presence of biomat with 8 hours of daily irradiation. In the transformation pathway, photo- and biotransformation reactions and structural changes in the molecules are indicated in orange and green, respectively.

376

Transformation of acyclovir

377

378 In contrast to abacavir, the transformation of acyclovir was dominated by microbial

379 processes (Fig. 5), with biotransformation resulting in the formation of acyclovir

380 carboxylate, which was not susceptible to further microbial transformation. These results

381 are consistent with previous biotransformation experiments conducted with acyclovir in

382 sewage sludge.[41]

383 In the absence of biomat material, exposure of wetland water to simulated sunlight

384 resulted in formation of two main photo-TPs (*i.e.*, TP257 and TP223). HRMS analysis

385 indicated that TP257 contains two additional oxygen atoms on the guanine moiety, as

17

evidenced by the detection of fragment m/z 184 instead of m/z 152 (Table S8; Fig. S16). Photosensitized degradation of guanine and guanosine occurs by reaction with excited triplet states, $^1O_2$, $^{\bullet}OH$ or $^{\bullet}CO_3^-$.[42,43] The main product of the reaction of guanine with $^1O_2$ has been identified as spiroiminodihydantoin.[44-46] To assess the role of $^1O_2$ in the phototransformation of acyclovir in wetland water, experiments were conducted in both H_2O and D_2O in the presence of the $^1O_2$ sensitizer Rose Bengal (Fig. 5). Lifetimes of $^1O_2$ in D_2O are more than an order of magnitude higher than in H_2O [39] and faster transformation of acyclovir in D_2O confirmed the role of $^1O_2$ in the indirect photolysis of acyclovir. In addition, the yield of TP257 increased in D_2O. Due to its photochemical properties, acyclovir is likely to undergo self-sensitation via photoexcitation and subsequent formation of $^1O_2$ as shown for guanine and guanosine.[48-50] For the second acyclovir photo-TP (TP223), HRMS analysis indicated the loss of two protons, most likely from the side chain, as evidenced by the detection of fragments m/z 152, 135 and 110, suggesting that the guanine moiety remained unchanged (Table S8). Additional information obtained from the fragmentation of the side chain was inconclusive but indicated oxidation of the terminal alcohol to the corresponding aldehyde via reaction with $^{\bullet}OH$.[51]

Results from the 72h simulated sunlight experiments conducted in the presence of the biomat revealed a steady decrease of acyclovir during light and dark periods, indicating the dominance of biotransformation processes (Fig. 5b). However, biotransformation of acyclovir was significantly faster in the sunlight experiments compared to dark controls (Fig. 5a&b) suggesting that the higher oxygen concentrations and the elevated pH values that occurred when microorganisms in the biomat were undergoing photosynthesis played a role in the biotransformation processes.[10] In the presence of simulated sunlight, production of the two phototransformation products (i.e., TP257 and TP224) was observed. No significant removal of TP257 was detected during dark periods, suggesting limited biotransformation via oxidation of the terminal hydroxyl-group of the side chain. Although the exact reason for this is unknown, a plausible explanation is that the structural modifications of the guanine core moiety prevented enzymatic oxidation of TP257. In contrast, concentrations of TP223 decreased in the dark. For the biotransformation product (i.e., acyclovir carboxylate), increasing concentrations were only observed during dark periods, whereas its concentration decreased upon exposure to sunlight. This

417 indicates that the compound was transformed further by photolytic processes, most likely
418 via the same mechanisms as acyclovir. This was confirmed by additional irradiation
419 experiments with acyclovir carboxylate in wetland water (results not shown).
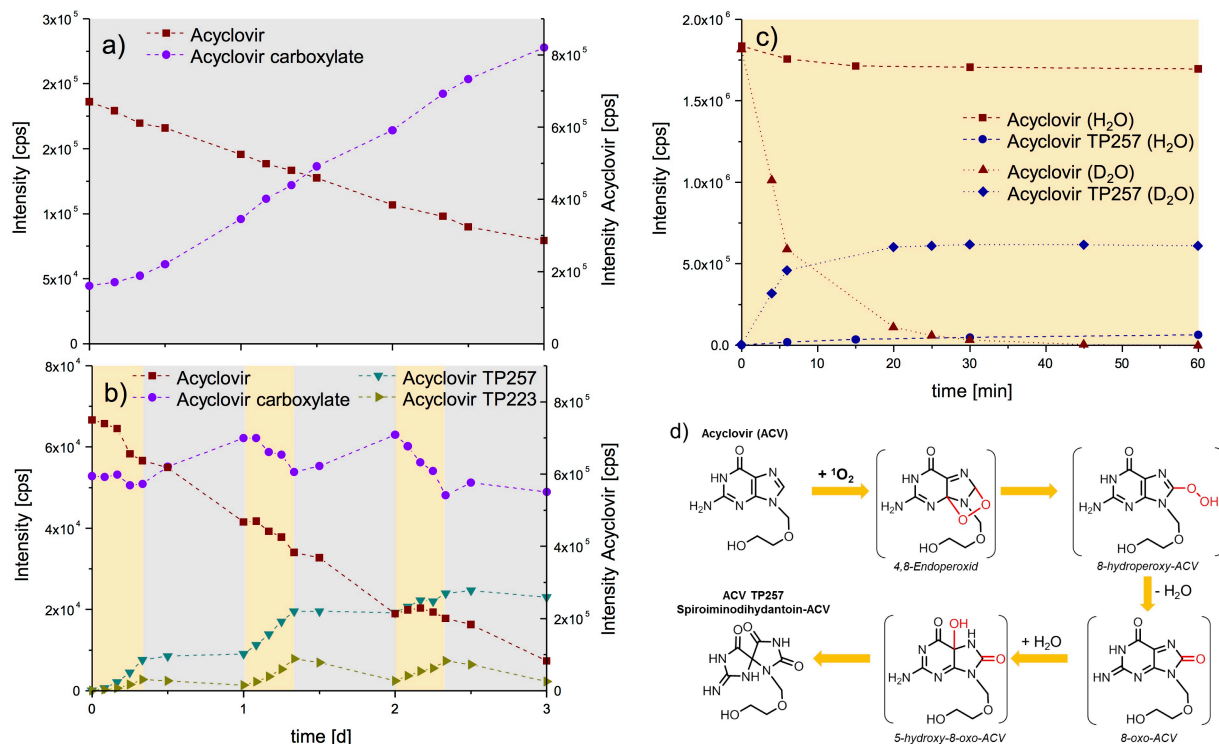420

Figure 5. Transformation of acyclovir in the presence of biomat in the dark (a) in combined photo- and biotransformation experiments (b), as well as formation of TP257 via reaction of acyclovir with $^1O_2$ in D_2O and H_2O using Rose Bengal as photosensitizer (c) and its proposed phototransformation pathway (d). The occurrence of acyclovir carboxylate at t_0 in (a) and (b) is due to its emission by the WWTP that feeds the wetland.

421

Transformation of zidovudine, lamivudine and emtricitabine

423 MS spectra of the phototransformation products of emtricitabine, lamivudine and
424 zidovudine indicated structural changes at different positions on the molecules (Table S9-
425 S11). For lamivudine and emtricitabine, HRMS analysis revealed oxidation of the riboside
426 moiety (lamivudine TP245 and emtricitabine TP263), most likely via S-oxidation. This was
427 confirmed by comparison with commercially available reference standards. Addition of
428 H_2O to the 5-fluoro-cytosine moiety was observed for emtricitabine (emtricitabine TP265).
429 Experiments conducted with the fluorine-free analogue lamivudine illustrate the
430 importance of fluorine substitution: the F-moiety increases the light absorbance at

19

431 wavelengths > 300 nm (Fig. S2) for emtricitabine and leads to faster photodegradation
432 (Figure 1, Table S5). Emtricitabine TP265 was formed via hydration of the double bond of
433 the 5-fluorocytosine moiety, yielding a hydroxyl-group at position C6. For zidovudine,
434 observed phototransformations were mainly attributable to the photolability of the azido
435 moiety. Formation of zidovudine TP239 can be explained by cleavage of N_2, yielding a
436 nitrene intermediate, which reacts further via intramolecular C-H insertion to an
437 aziridine.[52,53] Subsequent nucleophilic attack of the aziridine by water leads to the
438 hydroxylation of the C atom in β-position or the formation of a hydroxylamine (zidovudine
439 TP257).[52,54] Results from HRMS analysis of zidovudine TP221 were inconclusive but
440 indicated cleavage of N_2 and H_2O from the furanosyl moiety.

441 In addition, photolytic cleavage of the nitrogen-carbon bond between the DNA base
442 moieties and the riboside analogue side chains was observed for all three compounds,
443 resulting in formation 5-fluoro-cytosine (emtricitabine TP129), cytosine (lamivudine
444 TP111) and thymine (zidovudine TP126). None of these TPs were detected in sunlight
445 experiments in the presence of biomat (Fig. S21-22), indicating that they were rapidly
446 transformed, most likely via microbial processes. For zidovudine, this was confirmed by
447 additional biodegradation experiments with the photo-TPs (i.e., thymine, TP239, TP257),
448 showing the rapid elimination of thymine (Fig. S22). Considering the importance of both
449 thymine and cytosine as DNA building blocks, it is likely that they were incorporated into
450 the microbial biomass. The fate of 5-fluorocytosine remains unclear.

451 Similar to abacavir and acyclovir, biotransformation of emtricitabine, lamivudine and
452 zidovudine was shown to result in the formation of carboxylated TPs via oxidation of the
453 terminal alcohol as observed previously for abacavir and acyclovir (Fig. S13). As
454 carboxylated TPs are expected to follow the same phototransformation mechanisms as the
455 parent compounds, the interactions of photo- and biotransformation reactions is likely to
456 result in their complete elimination via mineralization and/or microbial uptake (Fig. 6).
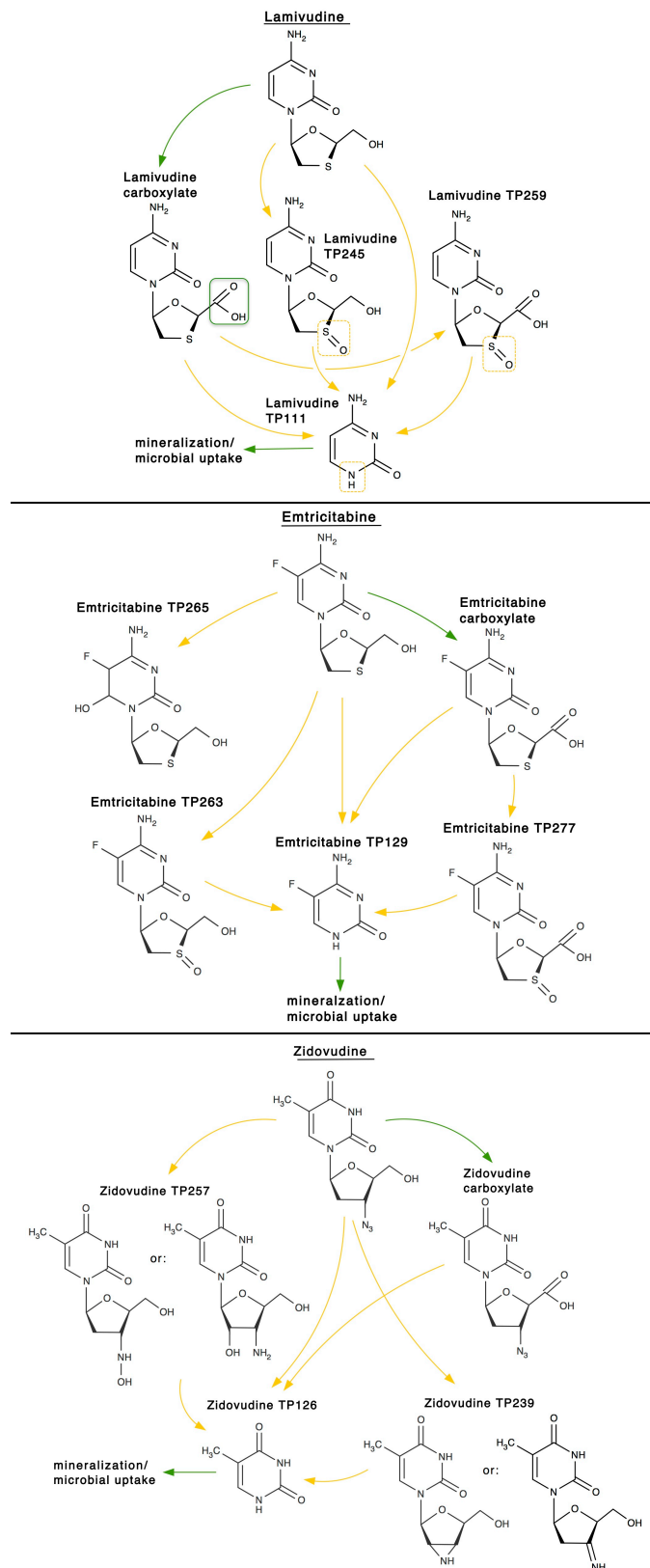
457
458
459
460

Figure 6. Proposed photo- and biodegradation pathway of lamivudine (top), emtricitabine (middle) and zidovudine (bottom) in open-water wetland cells. Orange and green

461

462 *Environmental implications*

463 The differences between kinetics and transformation product formation in the presence

464 and absence of the biomat highlight the complexity of transformation reactions that lead to

465 the removal of trace organic contaminants in open water unit process wetlands and other

466 sunlit waters. Attempts to predict the environmental fate of organic contaminants in these

467 systems requires an understanding of both processes as well as their potential interactions.

468 Identification of TPs showed that bio- and phototransformation reactions took place at

469 different positions of the antiviral molecules. Phototransformation of biodegradation

470 products was found to occur at the same location as in the parent compound. As a result,

471 mechanisms and kinetics were similar to those observed for parent antiviral compounds.

472 This is important because carboxylate biodegradation products are typically present in

473 much higher concentrations in biological treated wastewater compared to parent

474 compounds.[40] In contrast, biodegradation kinetics of phototransformation products of

475 antiviral drugs differed substantially from that observed for the parent compound even

476 though the site of enzymatic oxidation did not change. This can be explained by differences

477 in enzyme affinities and steric hindrance. For example, phototransformation of acyclovir

478 created a transformation product (TP257) that was not susceptible to biotransformation

479 by microorganisms that could oxidize the parent compound in the dark.

480 Combining kinetic studies with investigations of transformation product formation

481 provides a better understanding of mechanisms relevant for the removal of trace organic

482 contaminants in sunlit waters. By conducting biotransformation studies in the presence

483 and absence of light it is possible to assess interactions between transformation processes

484 and the likelihood that complete mineralization of trace organic contaminants will occur.

485 These data also suggest that relative ratios of antiviral compounds and their

486 transformation products might be useful as *in situ* probes to assess the relative importance

487 of microbial and photochemical transformation pathways. This study highlights the need to

488 consider the formation of different transformation products in sunlit and light-shaded

489 systems and the possibility of using knowledge of the reactivity of specific moieties in

22

490 chemical fate assessment. Considering the variety of formed transformation products,

491 there is a need for appropriate risk assessment tools to assess potential adverse effects of

492 transformation products with unknown toxicities on aquatic ecosystems. Additional field

493 studies may further confirm these laboratory microcosm results and help to assess the

494 suitability of the approach for determining the relative importance of individual

495 transformation processes.

496

497 **Supporting Information**

498 Additional information on sample analysis, UV spectra of antiviral drugs,

499 phototransformation kinetics plots, determination of indirect photolysis reaction rate

500 constants, quantum yields, steady state concentrations of reactive intermediates in wetland

501 water, experiments with DNA model compounds, MS^n fragments of transformation

502 products, formation and fate of abacavir photo-TPs by different reactive intermediates,

503 results of combined bio- and phototransformation experiments with emtricitabine,

504 lamivudine and zidovudine is available free of charge via the Internet at

505 http://pubs.acs.org.

506

513

514 **References**

515 (1)   Burrows, H.Dl; Canle, M.; Santaballa, J.A.; Steenken, S. Reaction pathways and
516   mechanisms of photodegradation of pesticides. *J . Photoch. Photobio. B* **2002**, 67(2),
517   71-108.
518 (2)   Boreen, A.L.; Arnold, W.A.; McNeill, K. Photodegradation of pharmaceuticals in the
519   aquatic environment: A review. *Aquat. Sci.* **2003**, 65(4), 320-341.
520 (3)   Halling-Sorensen, B.; Nielsen, S.N.; Lanzky, P.F.; Ingerslev, F.; Lutzhoft, H.C.H.;
521   Jorgensen, S.E. Occurrence, fate and effects of pharmaceutical substances in the
522   environment - A review. *Chemosphere* **1998**, 36(2), 357-394.

523   (4)   Onesios, K.M.; Yu, J.T.; Bouwer, E.J. Biodegradation and removal of pharmaceuticals
524   and personal care products in treatment systems: a review. *Biodegradation* **2009**,
525   20(4), 441-466.
526   (5)   Lam, M.W.; Mabury, S.A. Photodegradation of the pharmaceuticals atorvastatin,
527   carbamazepine, levofloxacin, and sulfamethoxazole in natural waters. *Aquat. Sci.*
528   **2005**, 67(2), 177-188.
529   (6)   Chiron, S.; Minero, C.; Vione, D. Photodegradation processes of the antiepileptic drug
530   carbamazepine, relevant to estuarine waters. *Environ. Sci. Technol.* **2006**, 40(19),
531   5977-5983.
532   (7)   De Laurentiis, E.; Chiron, S.; Kouras-Hadef, S., Richard, C.; Minella, M.; Maurino, V.;
533   Minero, C.; Vione, D. Photochemical fate of carbamazepine in surface freshwaters:
534   Laboratory measures and modeling. *Environ. Sci. Technol.* **2012**, 46(15), 8164-8173.
535   (8)   Kaiser, E.; Prasse, C.; Wagner, M.; Broeder, K.; Ternes, T.A. Transformation of
536   oxcarbazepine and human metabolites of carbamazepine and oxcarbazepine in
537   wastewater treatment and sand filters. *Environ. Sci. Technol.* **2014**, 48(17), 10208-
538   10216.
539   (9)   Jasper, J.T.; Nguyen, M.T. Jones, Z.L.; Ismail, N.S.; Sedlak, D.L., Sharp, J.O.; Luthy, R.G.,
540   Horne, A.J.; Nelson, K.L. Unit process wetlands for removal of trace organic
541   contaminants and pathogens from municipal wastewater effluents. *Environ. Engin.*
542   *Sci.* **2013**, 30(8), 421-436.
543   (10)   Jasper, J.T.; Sedlak, D.L. Phototransformation of wastewater-derived trace organic
544   contaminants in open-water unit process treatment wetlands. *Environ. Sci. Technol.*
545   **2013**, 47(19), 10781-10790.
546   (11)   Nguyen, M.T.; Silverman, A.I.; Nelson, K.L. Sunlight inactivation of MS2 coliphage in
547   the absence of photosensitizers: Modeling the endogenous inactivation rate using a
548   photoaction spectrum. *Environ. Sci. Technol.* **2014**, 48(7), 3891-3898.
549   (12)   Silverman, A.I.; Nguyen, M.T.; Schilling, I.E.; Wenk, J.; Nelson, K.L. Sunlight
550   inactivation of viruses in open-water unit process treatment wetlands: Modeling
551   endogenous and exogenous inactivation rates. *Environ. Sci. Technol.* **2015**, 49(5),
552   2757-2766.
553   (13)   Jasper, J.T.; Jones, Z.L.; Sharp, J.O.; Sedlak, D.L. Biotransformation of trace organic
554   contaminants in open-water unit process treatment wetlands. *Environ. Sci. Technol.*
555   **2014**, 48(9), 5136-5144.
556   (14)   Jasper, J.T.; Jones, Z.L.; Sharp, J.O.; Sedlak, D.L. Nitrate removal in shallow, open-
557   water treatment wetlands. *Environ. Sci. Technol.* **2014**, 48(19), 11512-11520.
558   (15)   Wood, T.P.; Duvenage, C.S.J.; Rohwer, E. The occurrence of anti-retroviral
559   compounds used for HIV treatment in South African surface water. *Environ. Pollut.*
560   **2015**, 199, 235-243.
561   (16)   Peng, X.; Wang, C.; Zhang, K.; Wang, Z.F.; Huang, Q.X.; Yu, Y.Y.; Ou, W.H. Profile and
562   behavior of antiviral drugs in aquatic environments of the Pearl River Delta, China.
563   *Sci. Total Environ.* **2014**, 466, 755-761.
564   (17)   Prasse, C.; Schluesener, M.P.; Schulz, R.; Ternes, T.A. Antiviral drugs in wastewater
565   and surface waters: A new pharmaceutical class of environmental relevance?
566   *Environ. Sci. Technol.* **2010**, 44(5), 1728-1735.

567 (18) Azuma, T.; Nakada, N.; Yamashita, N.; Tanaka, H. Synchronous dynamics of observed
568 and predicted values of anti-influenza drugs in environmental waters during a
569 seasonal influenza outbreak. *Environ. Sci. Technol.* **2012**, 46(23), 12873-12881.
570 (19) Wommack, K.E.; Colwell. R.R. Virioplankton: Viruses in aquatic ecosystems.
571 *Microbiol. Mol. Biol. R.* **2000**, 64(1), 69-114.
572 (20) Dulin, D.; Mill, T. Development and evaluation of sunlight actinometers. *Environ. Sci.*
573 *Technol.* **1982**, 16(11), 815-820.
574 (21) Grebel, J. E.; Pignatello, J. J.; Mitch, W. A. Sorbic acid as a quantitative probe for the
575 formation, scavenging and steady-state concentrations of the triplet-excited state of
576 organic compounds. *Water Res.* **2011**, 45(19), 6535–6544.
577 (22) Boreen, A.L.; Edhlund, B.L.; Cotner, J.B.; McNeill, K. Indirectphotodegradation of
578 dissolved free amino acids: The contribution ofsinglet oxygen and the differential
579 reactivity of DOM from varioussources. *Environ. Sci. Technol.* **2008**, 42(15),
580 5492–5498.
581 (23) Packer, J. L.; Werner, J.J.; Latch, D.E.; McNeill, K.; Arnold, W.A. Photochemical fate of
582 pharmaceuticals in the environment: Naproxen,diclofenac, clofibric acid, and
583 ibuprofen. *Aquat. Sci.* **2003**, 65(4), 342–351.
584 (24) Vione, D.; Khanra, S.; Man, S.C.; Maddigapu, P.R.; Das, R.; Arsene, C.; Olariu, R.-I.;
585 Maurino, V.; Minero, C. Inhibition vs. enhancement of the nitrate-induced
586 phototransformation of organic substrates by the (OH)-O-center dot scavengers
587 bicarbonate and carbonate. *Water Res.* **2009**, 43(18), 4718-4728.
588 (25) Canonica, S.; Kohn, T.; Mac, M.; Real, F.J.; Wirz, J.; Von Gunten, U. Photosensitizer
589 method to determine rate constants for the reaction of carbonate radical with
590 organic compounds. *Environ. Sci. Technol.* **2005**, 39(23), 9182-9188.
591 (26) Bedini, A.; De Laurentiis, E.; Sur, B.; Maurino, V.; Minero, C.; Brigante, M.; Mailhot, G.;
592 Vione, D. Phototransformation of anthraquinone-2-sulphonate in aqueous solution.
593 *Photochem. Photobio. S.* **2012**, 11(9), 1445-1453.
594 (27) Zepp, R.G.; Hoigne, J.; Bader, H. Nitrate-induced photooxidation of trace organic
595 chemicals in water. *Environ. Sci. Technol.* **1987**, 21, 443-450.
596 (28) Burns, J.M.; Cooper, W.J.; Ferry, J.L.; King, D.W.; DiMento, B.P.; McNeill, K.; Miller, C.J.;
597 Miller, W.L.; Peake, B.M.; Rusak, S.A.; Rose, A.L.; Waite, T.D. Methods for reactive
598 oxygen species (ROS) detection in aqueous environments. *Aquat. Sci.* **2012**, 74(4),
599 683-734.
600 (29) Maddigapu, P.R.; Bedini, A.; Minero, C.; Maurino, V., Vione, D.; Brigante, M.; Mailhot,
601 G.; Sarakha, M. The ph-dependent photochemistry of anthraquinone-2-sulfonate.
602 *Photochem. Photobio. Sci.* **2010**, 9(3), 323-330.
603 (30) Sakkas, V.A.; Lambropoulou, D.A.; Albanis, T.A. Photochemical degradation study of
604 irgarol 1051 in natural waters: influence of humic and fulvic substances on the
605 reaction. *J. Photoch. Photobio. A* **2002**, 147(2), 135-141.
606 (31) Bouchoux, G.; Alcaraz, C.; Dutuit, O.; Nguyen, M.T. Unimolecular chemistry of the
607 gaseous cyclopropylamine radical cation. *J. Am. Chem. Soc.* **1998**, 120(1), 152-160.
608 (32) Cooksy, A.L.; King, H.F.; Richardson, W.H. Molecular orbital calculations of ring
609 opening of the isoelectronic cyclopropylcarbinyl radical, cyclopropoxy radical, and
610 cyclopropylaminium radical cation series of radical clocks. *J. Org. Chem.* **2003**,
611 68(24), 9441-9452.

612   (33)   Nakatani, K.; Dohno, C.; Saito, I. Design of a hole-trapping nucleobase: Termination
613   of DNA-mediated hole transport at N-2-cyclopropyldeoxyguanosine. *J. Am. Chem.*
614   *Soc.* **2001**, 123(39), 9681-9682.
615   (34)   Shao, F.W.; O'Neill, M.A.; Barton, J.K. Long-range oxidative damage to cytosines in
616   duplex DNA. *P. Natl. Acad. Sci. USA* **2004**, 101(52), 17914-17919.
617   (35)   Qin, X.Z.; Williams, F. Electron-spin-resonance studies on the radical cation
618   mechanism of the ring-opening of cyclopropylamines. *J. Am. Chem. Soc.* **1987**,
619   109(2), 595-597.
620   (36)   Paul, M.M.S.; Aravind, U.K.; Pramod, G.; Saha, A.; Aravindakumar, C.T. Hydroxyl
621   radical induced oxidation of theophylline in water: a kinetic and mechanistic study.
622   *Org. Biomol. Chem.* **2014**, 12(30), 5611-5620.
623   (37)   Goutailler, G.; Valette, J.C.; Guillard, C.; Paisse, O.; Faure, R. Photocatalysed
624   degradation of cyromazine in aqueous titanium dioxide suspensions: comparison
625   with photolysis. *J. Photoch. Photobio. A* **2001**, 141(1), 79-84.
626   (38)   Shaffer, C.L.; Morton, M.D.; Hanzlik, R.P. N-dealkylation of an N-cyclopropylamine by
627   horseradish peroxidase. Fate of the cyclopropyl group. *J. Am. Chem. Soc.* **2001**,
628   123(35), 8502-8508.
629   (39)   Cerny, M.A.; Hanzlik, R.P. Cytochrome P450-catalyzed oxidation of N-benzyl-N-
630   cyclopropylamine   generates   both   cyclopropanone   hydrate   and   3-
631   hydroxypropionaldehyde via hydrogen abstraction, not single electron transfer. *J.*
632   *Am. Chem. Soc.* **2006**, 128(10), 3346-3354.
633   (40)   Funke, J.; Prasse, C.; Ternes T.A. Identification and fate of transformation products of
634   antiviral drugs formed during biological wastewater treatment (submitted).
635   (41)   Prasse, C.; Wagner, M.; Schulz, R.; Ternes, T.A. Biotransformation of the antiviral
636   drugs acyclovir and penciclovir in activated sludge treatment. *Environ. Sci. Technol.*
637   **2011**, 45(7), 2761-2769.
638   (42)   Cadet, J.; Douki, T.; Gasparutto, D.; Ravanat, J.L. Oxidative damage to DNA: formation,
639   measurement and biochemical features. *Mutat. Res. - Fund. Mol. M.* **2003**, 531(1-2),
640   5-23.
641   (43)   Neeley, W.L.; Essigmann, J.M. Mechanisms of formation, genotoxicity, and mutation
642   of guanine oxidation products. *Chem. Res. Toxicol.* **2006**, 19(4), 491-505.
643   (44)   Cui, L.; Ye, W.; Prestwich, E.G.; Wishnok, J.S.; Taghizadeh, K.; Dedon, P.C.;
644   Tannenbaum S.R. Comparative analysis of four oxidized guanine lesions from
645   reactions of DNA with peroxynitrite, singlet oxygen and y-radiation. *Chem. Res.*
646   *Toxicol.* **2012**, 26(2), 195-202
647   (45)   Luo, W.; Muller, J.G.; Rachlin, E.M.; Burrows, C.J. Characterization of
648   spiroiminodihydantoin as a product of one-electron oxidation of 8-oxo-7,8-
649   dihydroguanosine. *Org. Lett.* **2000**, 2(5), 613-616.
650   (46)   Cadet, J.; Douki, T.; Ravanat, J.L. Oxidatively generated damage to the guanine moiety
651   of DNA: Mechanistic aspects and formation in cells. *Accounts Chem. Res.* **2008**, 41(8),
652   1075-1083.
653   (47)   Rodgers, M. A. J.; Snowden, P. T. Lifetime of $O_2(1\Delta g)$ in liquid water as determined by
654   time-resolved infrared luminescence measurements. *J. Am. Chem. Soc.* **1982**,
655   104(20), 5541-5543.

656   (48)   Mohammad, T.; Morrison, H. Evidence for the photosensitized formation of singlet
657   oxygen by UVB irradiation of 2'-deoxyguanosine 5'-monophosphate. *J. Am. Chem.*
658   *Soc.* **1996**, 118(5), 1221-1222.
659   (49)   Redmond, R.W.; Gamlin, J.N. A compilation of singlet oxygen yields from biologically
660   relevant molecules. *Photochem. Photobiol.* **1999**, 70(4), 391-475.
661   (50)   Torun, L.; Morrison, H. Photooxidation of 2'-deoxyguanosine 5'-monophosphate in
662   aqueous solution. *Photochem. Photobiol.* **2003**, 77(4), 370-375.
663   (51)   von Gunten, U. Ozonation of drinking water: Part I. Oxidation kinetics and product
664   formation. *Water Res.* **2003**, 37(7), 1443-1467.
665   (52)   Dunge, A.; Chakraborti, A.K.; Singh, S. Mechanistic explanation to the variable
666   degradation behaviour of stavudine and zidovudine under hydrolytic, oxidative and
667   photolytic conditions. *J. Pharmaceut. Biomed.* **2004**, 35(4), 965-970.
668   (53)   Gritsan, N.; Platz M. Photochemistry of azides: The azide/nitrene interface. In
669   *Organic Azides: Syntheses and Applications*; Bräse, S., Banert, K., Eds.; John Wiley &
670   Sons; 2010, pp 311-372.
671   (54)   Iwamoto, T.; Hiraku, Y.; Oikawa, S.; Mizutani, H.; Kojima, M.; Kawanishi, S. Oxidative
672   DNA damage induced by photodegradation products of 3'-azido-3'-deoxythymidine.
673   *Archives of Biochemistry and Biophysics.* 2003;416(2):155-163.
674